Double-Sampled Echo-Planar Imaging at 3 Tesla*

QING X. YANG,† STEFAN POSSE,‡ DENIS LE BIHAN,§ AND MICHAEL B. SMITH†·¶·‖

†*Department of Radiology (Center for NMR Research) and* ¶*Department of Cellular and Molecular Physiology, The Pennsylvania State University, College of Medicine, The Milton S. Hershey Medical Center, Hershey, Pennsylvania 17033;* ‡*Institute of Medicine, Research Center Juelich GmbH, D-52425 Juelich, Germany; and* §*Service Hospitalier Frederic Joilot, DRIPP, 4, Place du General Leclerc, 91401 Orsay Cedex, France*

A persistent artifact in the images acquired by the echo-planar imaging (EPI) method is the Nyquist or N/2 ghost which interferes with the image and reduces the signal-to-noise ratio (SNR). The Nyquist ghost is the result of the time-reversal asymmetry between the even and odd echoes. To eliminate this artifact, the authors present a double-sampled EPI (DSEPI) method in which echoes from each even and odd echo pair are equally phase encoded. The even and odd echoes are separately reconstructed into two distinct images which are then added together. The DSEPI method has been applied to human brain at 3.0 T and shown to be a simple and effective way to eliminate the Nyquist ghost and restore image SNR loss. © 1996 Academic Press, Inc.

INTRODUCTION

The echo-planar imaging (EPI) technique (*1*) has been an effective method in performing functional magnetic resonance imaging (f MRI) (*2–6*). EPI images, however, are sensitive to magnetic-field inhomogeneities and various hardware-related artifacts. One of the persistent artifacts is the so-called Nyquist or N/2 ghost which is centered at half of the field of view away from the image in the phase-encoding dimension. The Nyquist ghost interferes with the image where overlaps occur and reduces the image signal-to-noise ratio (SNR). For f MRI, the interference of the ghost with the possible functionally activated regions may cause ambiguities in data interpretation.

In the blipped EPI method (*7*), k-space is sampled by switching the readout gradient back and forth rapidly with opposite polarity, generating a series of gradient-recalled echoes. A typical conventional EPI k-space trajectory is shown in Fig. 1a. The even-numbered echoes and odd-numbered echoes in the echo train are produced by readout gradients with opposite polarity. One set of echoes needs to be time reversed before Fourier reconstruction. This requires that all the echoes possess perfect time-reversal symmetry.

As illustrated in Fig. 1b, any time-reversal asymmetry in shape and/or in position between the even and odd echoes results in a double-period modulation along the phase direction in k-space which causes the Nyquist ghost in the reconstructed image.

Misalignment between the even and odd echoes can be reduced partially by tedious adjustment of the strength of the pre-readout gradient and the timing of digitization, or by postprocessing with the aid of an internal or external reference scan (*8–12*). There is, however, no effective way to correct the shape asymmetry between the even and odd echoes. The shape asymmetry between the even and odd echoes is caused by the time-reversal asymmetry of the gradient waveform, the gradient eddy currents, and the modulations due to the static-magnetic-field inhomogeneities.

The Nyquist ghost is rooted in the EPI data acquisition process and cannot be eliminated completely, although the artifacts may be smaller for some MRI systems equipped with well-built gradients at 1.5 T or lower field strength. The asymmetry caused by magnetic-field-inhomogeneity modulation becomes more serious at high field strength due to stronger magnetic susceptibility effects. Feinberg *et al.* have proposed an acquisition method (AB-EST) in which only the echoes corresponding to one polarity of the readout gradient were used for image reconstruction (*13*). In ABEST, the source of the Nyquist ghost was eliminated, but the time to reverse the echo, while shortened with a stronger gradient pulse, was not utilized for data acquisition. In ultra-fast imaging, it is more efficient to acquire the signal during the entire acquisition window (about 100 ms) to maximize the image pixel resolution and/or the SNR. Johnson *et al.* (*14*) suggested that the even and odd echoes could be sampled and processed separately and the images added after processing to increase image SNR. This procedure, which was experimentally implemented by Chapman *et al.* using two separated but interleaved acquisitions (*15*), is more efficient than ABEST for generating Nyquist-ghost-free images.

The recent development in f MRI field has stimulated a broad interest in ultra-fast imaging at higher field strengths.
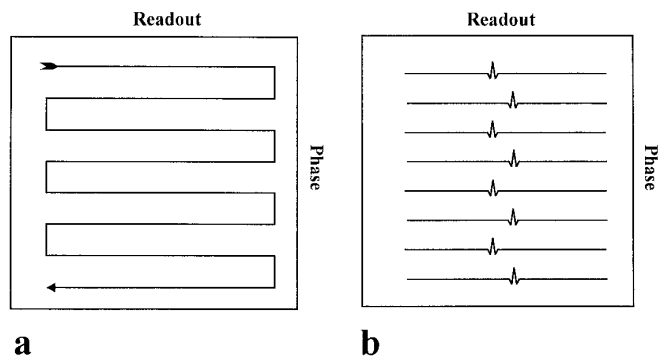
FIG. 1. (a) In the conventional EPI technique, adjacent lines of the trajectory are produced by readout gradients of opposite polarity. (b) Any time-reversal asymmetry of the gradient waveform will destroy the time-reversal symmetry between the even and odd echoes. After time reversal of one set of the echoes, the differences between the even and odd echoes introduce a double-period modulation in the phase direction of k space which causes the Nyquist ghost in the conventional EPI images.

Single-shot EPI at higher magnetic field strength is the most desirable method for dynamic f MRI. However, the stronger magnetic susceptibility effect at high field strengths also aggravates the artifacts in the conventional EPI images. Thus, experimental assessment of the trade-offs of various EPI acquisition methods at high field strength is in order. In this report, we extend Johnson's idea and present a double-sampled EPI (DSEPI) technique in an effort to explore effective single-shot data acquisition methods. The experimental results obtained at 3.0 T suggest that DSEPI is an efficient acquisition method for high field to effectively eliminate the Nyquist ghost and restore the SNR loss.

THEORY

The gradient-timing diagram for DSEPI is shown in Fig. 2a. In data acquisition, the major distinction between DSEPI and conventional blipped EPI is that the phase-encoding gradient blips occur on every other echo rather than on every echo. Data acquired in the even and odd echo pairs have the same phase encoding. The resultant DSEPI k-space trajectory, as shown in Fig. 2b, sweeps forward and back along the same path, and then proceeds to the next line. Therefore, each line in k-space is double sampled with the positive and negative readout gradients. The even and odd echoes are then reconstructed separately, generating two distinct magnitude images. Neither image contains a Nyquist ghost. The spatial frequency information contained in this image pair is essentially the same except for a temporal shift of one echo time, which in our case is 512 μs. This time shift produces an insignificant difference in T_2^* weighting and a global phase difference which does not affect the final magnitude image. Thus, these two images can be added together to produce the final DSEPI image.

Experimental parameters must be considered carefully when comparing the DSEPI technique with conventional EPI. For an image of a given pixel resolution, DSEPI acquires twice as many data points as conventional EPI. In order to maintain the same acquisition time as conventional EPI, it is necessary to double the bandwidth (oversample). Oversampling requires a doubling of the gradient strength and a shortening of the gradient rise times. The increased bandwidth reduces the SNR of each even and odd echo image by a factor of $\sqrt{2}$. This SNR loss is recovered by adding both images together (signal averaging), which yields the same SNR as that of conventional EPI.

DSEPI can also be performed without oversampling by doubling the acquisition time and maintaining the same bandwidth, gradient strength, and rise time as conventional EPI. In this case, the SNR of the combined DSEPI image increases by a factor of $\sqrt{2}$ at the expense of stronger off-resonance effects. Performing DSEPI with oversampling
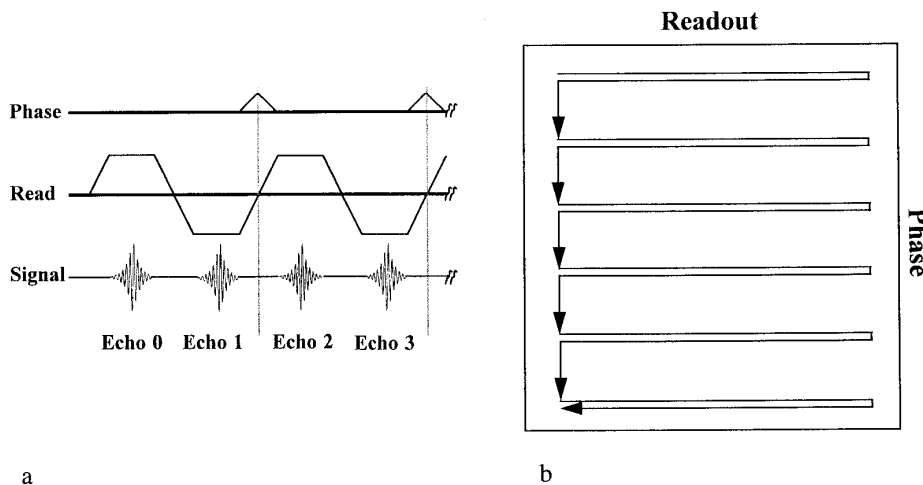
FIG. 2. The timing diagram of DSEPI (a) and the corresponding k-space trajectory (b). In the DSEPI-with-oversampling method, each line in k space is sampled twice with positive and negative readout gradient at a sampling rate twice that of conventional blipped EPI.

may be preferred at higher magnetic-field strengths where the susceptibility effects are stronger. Increasing image acquisition time is not desirable. DSEPI without oversampling may be a suitable trade-off at lower magnetic-field strengths since it improves the SNR and the susceptibility effects are weaker. In both cases, the k-space coverage is maintained as in conventional EPI. Since the ghosts represent the part of the acquired signal which is incorrectly reconstructed, the image SNR is decreased by the ghosting. This incorrectly reconstructed signal is restored by DSEPI to the correct region of the final image.

METHODS

The gradient-echo (GE) DSEPI method was implemented on a Bruker Medspec S300 3.0 T, 90 cm, whole-body imager with an actively shielded head gradient insert with a maximum strength of 3.0 G/cm (Bruker Instruments, Inc., Karlsruhe, Germany). The phantom sample used in this study was a 16 cm diameter sphere containing 0.5 mM $CuSO_4$ solution. Human brain images in this study were acquired on normal volunteers. Informed consent was obtained from all the subjects. All images were acquired with a 20 cm field of view (FOV), a 6 mm slice thickness, and 64×64 pixel resolution. The DSEPI images were obtained by acquiring 64 even and 64 odd echoes in 65.5 ms with a bandwidth of 125 kHz. The even and odd echoes were separated and reconstructed individually by a Bruker-supplied Fourier reconstruction routine without any other postprocessing. For comparison purposes, both 32.8 and 65.5 ms conventional blipped GE EPI images were acquired with a bandwidth of 125 and 62.5 kHz, respectively. The conventional GE EPI images were acquired with optimized echo positions and further postprocessed with reference prescans that were acquired by turning off the phase-encoding gradient prior to the acquisition of the EPI image. A trapezoidal waveform was used for the readout gradient. In order to compare quantitatively the images acquired with different bandwidths, the k-space coverage was kept constant. For the 125 kHz images, the readout gradient was 512 μs in length and 1.47 G/cm in strength with a rise time of 60 μs. For the 62.5 kHz images, the readout gradient was 1024 μs in length and 0.73 G/cm in strength with a rise time of 120 μs. The effective TE was maintained at 35.0 ms for all the images. Brief manual first-order shimming over the entire phantom or head was performed prior to image acquisition. The full width at half-height of the water spectrum from both phantom and human brains was maintained at approximately 20 Hz.

RESULTS

Figure 3 shows the images (64×64) of a 16 cm diameter spherical phantom acquired in 65.5 ms by both conventional EPI and DSEPI. To demonstrate the effect on ghost reduc-

tion, the corresponding background-highlighted images are also shown below each image. The Nyquist ghosts which are quite prominent in the conventional EPI image are essentially eliminated in the DSEPI images. To assess the ghost reduction, the ratio of averaged pixel intensity in the ghost region to the image (GSR) is used. Regions where the ghost and image were combined due to overlap were excluded from both calculations of GSR and SNR. The GSR in the EPI image is 0.14 or 14%. For the DSEPI image there is no ghost by definition. The average pixel intensity in the corresponding ghost region in the DSEPI image is equal to the noise level. The SNR is 58 for the DSEPI image and 51 for the conventional EPI image. The SNR increase for the DSEPI image is mainly due to ghost suppression.

Figure 4 shows three 64×64 axial brain images, along with their background-highlighted images. Figure 4a is a conventional EPI image acquired in 32.8 ms with a bandwidth of 125 kHz. Figure 4b is a conventional EPI image acquired in 65.5 ms with a bandwidth of 62.5 kHz, and Fig. 4c depicts a DSEPI image acquired in 65.5 ms with a bandwidth of 125 kHz. The GSR and SNR of these images are also shown. Note that Fig. 4c represents a DSEPI-with-oversampling image when compared with the 62.5 kHz bandwidth conventional EPI image in Fig. 4b, and a DSEPI-without-oversampling image when compared with the 125 kHz conventional images in Fig. 4a. For Fig. 4, the ghost reduction by DSEPI is evident. The EPI images in Fig. 4 are normally considered to be acceptable, but their GSRs are still as large as 16 to 30%, while in the DSEPI image there are no observable ghosts. The ghosts in the EPI images are more prominent along the edges where they are most likely to overlap with the image.

DISCUSSION

The point spread function of an EPI image is inherently weighted by T_2^*. The T_2^* decay during the echo formation read time creates an asymmetry in each echo, and a shape asymmetry between the even and odd echoes with time reversal prior to the reconstruction. In addition to the T_2^* signal attenuation, the local field gradients also cause echo shift and broadening in readout, and phase errors in phase-encoding directions, respectively (*16, 17*). These errors are accumulative and asymmetric relative to the encoding gradient polarity. The time-reversal asymmetry caused by field inhomogeneities becomes larger for later echoes which are normally phase encoded with higher spatial frequencies. Thus, Nyquist ghosts become larger in the peripheral regions of the brain where the B_0 field is less homogeneous. With conventional EPI, Nyquist ghosts can be only partially reduced by aligning the even and odd echoes or by a linear phase correction with the aid of a reference prescan. Higher magnetic-field strength is desirable for f MRI because of the enhancement in SNR

EPI   DSEPI

GSR = 14%
SNR = 51

GSR < 1.7%
SNR = 58
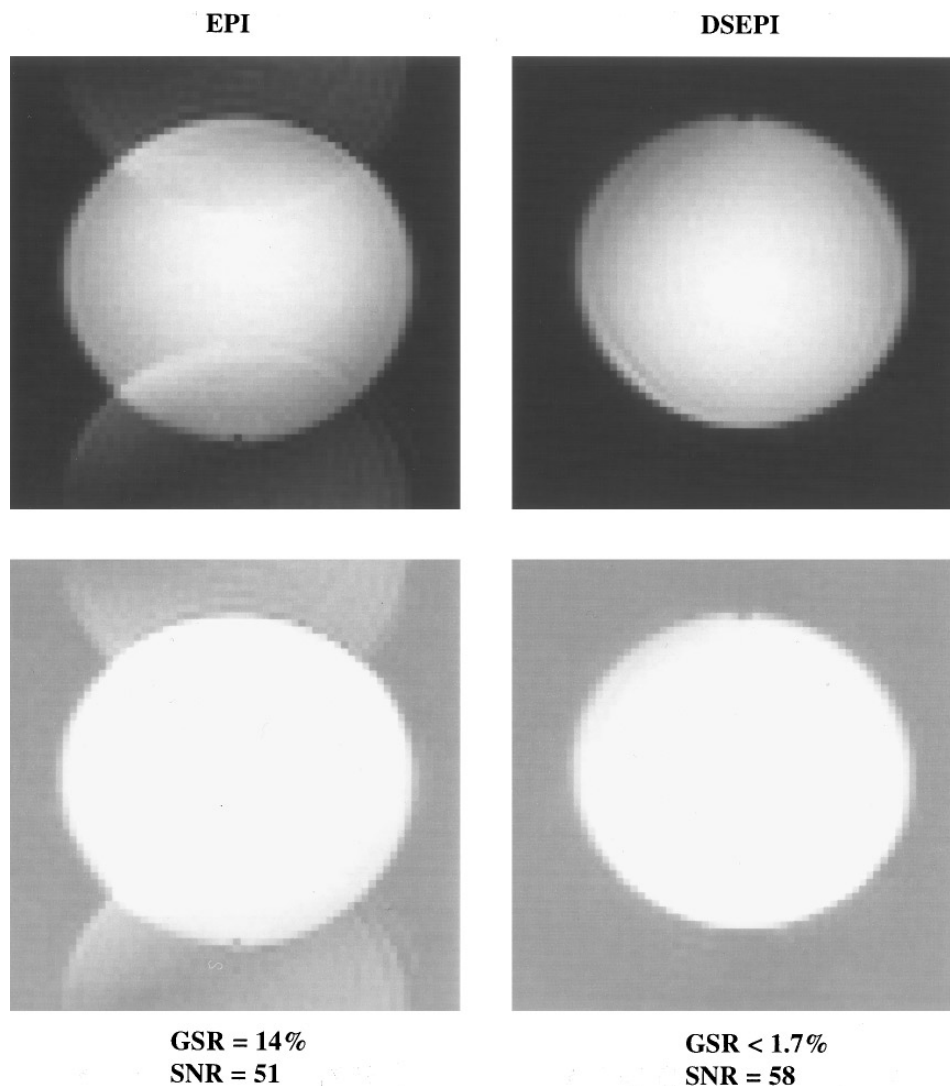
FIG. 3. Axial 64 × 64 images of a 16 cm diameter sphere acquired in 65.5 ms by conventional gradient-echo EPI with 62.5 kHz bandwidth and by DSEPI with 125 kHz bandwidth. The Nyquist ghost in the conventional EPI image is eliminated in the DSEPI image.

and the blood-oxygen-level-dependent (BOLD) contrast. With conventional EPI, the stronger magnetic susceptibility effects at higher field strengths also enhance Nyquist ghosts since time-reversal asymmetry caused by field inhomogeneities becomes more prominent. DSEPI offers advantages for f MRI at higher field strengths by eliminating ghosts.

For conventional EPI images, the SNR in the image with a 62.5 kHz bandwidth (Fig. 4b) is 36% higher than that with a 125 kHz bandwidth (Fig. 4a). The SNR in the DSEPI brain image with 125 kHz bandwidth (Fig. 4c) is 6% greater than that of the 62.5 kHz bandwidth EPI image (Fig. 4b). For phantom images in Fig. 3, the SNR of the DSEPI image with 125 kHz bandwidth is 12% greater than that of the 62.5 kHz bandwidth EPI image. This SNR improvement due to ghost suppression by DSEPI is significant, considering that

the NMR signal from a human subject by single excitation is limited.

DSEPI significantly simplifies data acquisition and postprocessing and allows acquisition of consistent ghost-free images at 3.0 T. EPI imaging normally requires lengthy periods of checking and adjusting parameters to optimize the echo position. Patient movement between the prescan and image acquisition could also severely degrade image quality. DSEPI requires neither adjustment of experimental parameters nor a prescan, and thus allows one to take full advantage of EPI as a signal-shot technique. EPI acquisition methods are inherently sensitive to field inhomogeneities because of their slow effective acquisition rate in the phase-encoding direction. Phase errors due to field inhomogeneities lead to geometry distortions in the image if present in the image data. The image distortions may be even worse if

GSR = 30%
SNR = 25

a

GSR = 16%
SNR = 34

b

GSR < 2.8%
SNR = 36

c
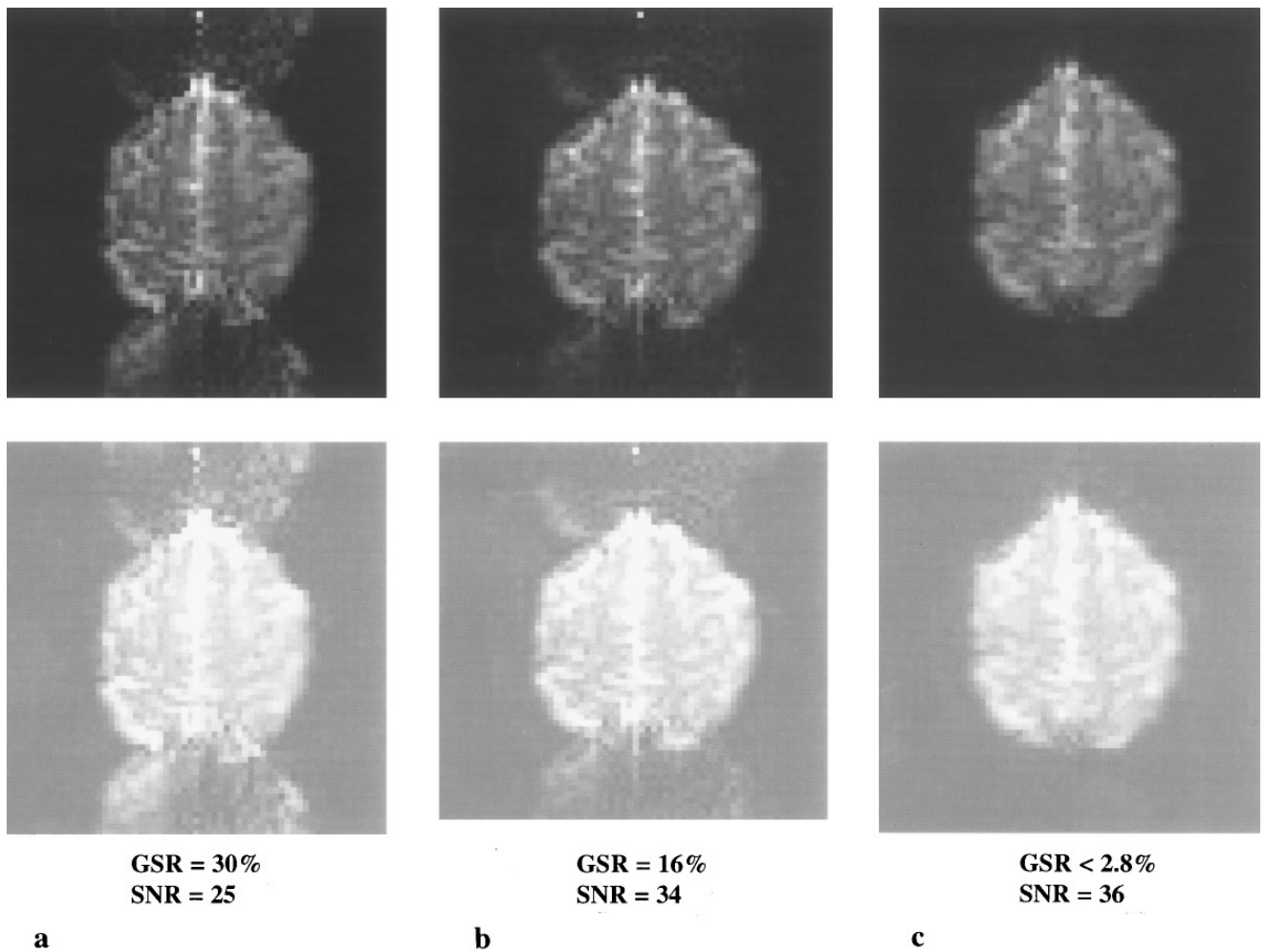
FIG. 4. Axial 64×64 brain images using conventional EPI acquired with a bandwidth and acquisition time of 125 kHz and 32.8 ms (a) and 62.5 kHz and 65.5 ms (b), and using DSEPI with a bandwidth and acquisition time of 125 kHz and 65.5 ms (c).

additional phase errors are present in the prescan data (*8*). Therefore, it is advantageous to avoid the use of prescans at high magnetic-field strength where field inhomogeneities due to the magnetic susceptibility effect are stronger.

Increasing the acquisition bandwidth requires a stronger gradient, which is a restriction associated with the use of the DSEPI-with-oversampling method. Gradient strength and rise time limit a wider implementation of the DSEPI technique at the present time. However, continued rapid developments in gradient technology should make stronger gradients more readily available in the near future. It is important that the dB/dt be maintained within the safety threshold when DSEPI with oversampling is considered. Similar restrictions also exist in the ABEST method, in which a stronger rewinding readout gradient is also used to increase the pixel resolution or reduce the acquisition time. For a given gradient strength, the stronger rewinding gradient in ABEST limits the minimal FOV and ultimate spatial resolution. As a fast imaging-data acquisition method it is

inefficient that the time to reverse the echoes is not utilized for data acquisition.

DSEPI without oversampling, on the other hand, has the advantage of SNR enhancement and the disadvantage of longer acquisition time which limits the image resolution and leads to stronger off-resonance artifacts. However, the acquisition time can be decreased, if desired, at the cost of sacrificing the SNR enhancement by combining DSEPI with the half-Fourier (*18*) acquisition method. Compared with conventional EPI in this case, the problems with longer acquisition time in DSEPI are overcome, while the advantage of complete elimination of the Nyquist ghost is still maintained. Thus, DSEPI with half-Fourier acquisition could be a desirable trade-off in many cases. The acquisition time can be reduced further by incorporating DSEPI into the multiple-shot EPI method (*19*). DSEPI is essentially a two-image-by-one-shot method, and therefore complementary to multiple-shot EPI. In all cases, the length of acquisition time is reduced, and the Nyquist-ghost problem is eliminated.

In summary, the DSEPI method virtually eliminates the Nyquist-ghost problem in the conventional EPI technique, which makes it a viable alternative acquisition method for high-speed imaging. We have tested this method *in vivo* at 3.0 T, and have demonstrated that the DSEPI method is a simple and effective way to eliminate the Nyquist ghost and improve SNR. The trade-offs associated with DSEPI, especially at high magnetic fields, make it a promising method for f MRI where high magnetic field is desirable. DSEPI relaxes the stringent demands on the gradient system and offers an opportunity to the investigators who currently do not have state-of-the-art actively shield gradients to acquire Nyquist-ghost-free images for their fast-imaging applications.

ACKNOWLEDGMENTS

REFERENCES

1. P. Mansfield, *J. Phys. C.* **10,** L55 (1977).

2. J. W. Belliveau, B. R. Rosen, H. L. Kantor, R. R. Rzedzian, D. N. Kennedy, R. C. McKinstry, J. M. Vevea, M. S. Cohen, I. L. Pykett, and T. J. Brady, *Magn. Reson. Med.* **14,** 538 (1990).

3. R. Turner, D. Le Bihan, C. T. W. Moonen, D. Despres, and J. Frank, *Magn. Reson. Med.* **22,** 159 (1991).

4. J. W. Belliveau, D. N. Kennedy, R. C. McKinstry, B. R. Buchbinder, R. M. Weisskoff, M. S. Cohen, J. M. Vevea, T. J. Brady, and B. R. Rosen, *Science* **254,** 716 (1991).

5. P. A. Bandettini, A. Jesmanowicz, E. C. Wong, and J. S. Hyde, *Magn. Reson. Med.* **30,** 161 (1993).

6. A. M. Blamire, S. Ogawa, K. Ugurbil, D. Rothman, G. McCarthy, J. Ellermann, F. Hyder, Z. Rattner, and R. G. Shulman, Abstracts of the Society of Magnetic Resonance in Medicine, 11th Annual Meeting, Berlin, p. 1823, 1992.

7. G. Johnson and J. M. S. Hutchison, *J. Magn. Reson.* **63,** 14 (1985).

8. E. C. Wong, Abstracts of the Society of Magnetic Resonance in Medicine, 11th Annual Meeting, Berlin, p. 4514, 1992.

9. A. Jesmanowicz, E. C. Wong, and J. S. Hyde, Abstracts of the Society of Magnetic Resonance in Medicine, 12th Annual Meeting, New York, p. 1239, 1993.

10. H. Bruder, H. Fischer, H.-E. Reinfelder, and F. Schmitt, *Magn. Reson. Med.* **23,** 311 (1992).

11. K. Sekihara and H. Kohno, *Magn. Reson. Med.* **5,** 485 (1987).

12. J. B. Mandeville, R. M. Weisskoff, and L. Garrido, Abstracts of the Society of Magnetic Resonance, Third Annual Meeting, Nice, France, p. 613, 1995.

13. D. A. Feinberg, R. Turner, P. D. Jakab, and M. von Kienlin, *Magn. Reson. Med.* **13,** 162 (1990).

14. G. Johnson, J. M. S. Hutchison, T. W. Redpath, and L. M. Eastwood, *J. Magn. Reson.* **54,** 473 (1983).

15. B. Chapman, R. Turner, R. J. Ordidge, M. Doyle, M. Cawley, R. Coxon, P. Glover, and P. Mansfield, *Magn. Reson. Med.* **5,** 246 (1987).

16. F. Farzaneh, S. J. Riederer, and N. J. Pelc, *Magn. Reson. Med.* **14,** 123 (1990).

17. S. Posse, *Magn. Reson. Med.* **25,** 12 (1992).

18. D. A. Feinberg, J. D. Hale, J. C. Watts, and L. Kaufman, *Radiology* **161,** 527 (1986).

19. K. Butts, S. J. Riederer, R. L. Ehman, and R. M. Thompson, C. R. Jack, *Magn. Reson. Med.* **31,** 67 (1994).